Further Numerical Calculations of the Circulation of the Atmosphere of Venus[1]

EUGENIA KÁLNAY DE RIVAS

Department of Meteorology, Massachusetts Institute of Technology, Cambridge 02139

(Manuscript received 6 December 1974, in revised form 27 February 1975)

ABSTRACT

The results of two-dimensional simulations of the deep circulation of Venus are presented. They prove that the high surface temperature can only be explained by the greenhouse effect, and that Goody and Robinson's dynamical model is not valid. Very long time integrations, up to a time comparable with the radiative relaxation time, confirm these results. Analytical radiative equilibrium solutions for a semi-grey atmosphere, both with and without an internal heat source, are presented. It is shown that the greenhouse effect is sufficient to produce the high surface temperature if $\tau_T^* \gg 100$ and $S = \tau_S^*/\tau_T^* \lesssim 0.005$. This result is still valid in the presence of an internal heat source of intensity compatible with observations.

A two-dimensional version of a three-dimensional model is used to test the validity of the new mechanism proposed by Gierasch to explain the 4-day circulation. Numerical experiments with horizontal viscosities $\nu_H = 10^{11} - 10^{12}$ cm^2 s^{-1} failed to show strong zonal velocities even for the case of large Prandtl numbers. It is observed that the dissipation of angular momentum introduced by the strong horizontal diffusion more than compensates for the upward transport of angular momentum due to the Hadley cell.

Preliminary three-dimensional calculations show a tendency to develop strong small-scale circulations.

1. Introduction

In the last fifteen years, two unexpected characteristics of the atmosphere of Venus have been discovered. One is the high surface temperature ($T_s \approx 750$ K) compared to the effective radiative temperature ($T_e \approx 230$ K). The other is the strong retrograde zonal motion of the upper atmosphere (the so-called "4-day circulation") with velocities of the order of 100 m s^{-1}. This is much larger than the planetary rotation speed at the equator which is less than 2 m s^{-1}, and also retrograde.

There have been several mechanisms offered to explain these phenomena, but they have not yet been proven to be right. One way to test their validity, and perhaps even to find other explanations, is to make a numerical simulation of the circulation of the atmosphere of Venus.

We developed several two-dimensional numerical atmospheric models for Venus, with the purpose of checking the validity of the two most important theories proposed to explain the high surface temperature, i.e., the greenhouse effect (Sagan, 1962; Pollack, 1969) and the dynamical model by Goody and Robinson (1966). Goody and Robinson proposed that even if solar radiation were absorbed at high levels, the horizontal temperature gradient would drive a large-scale circulation, which in turn would convect heat downward, maintaining the lapse rate close to adiabatic throughout the atmosphere.

We have reported some of the numerical results obtained (Kálnay de Rivas, 1973). When we used, as Goody and Robinson did, the Boussinesq approximation, we obtained results similar to theirs: a Hadley cell that penetrated the whole atmosphere developed, and the static stability remained very close to neutral. We then developed a quasi-Boussinesq or deep anelastic model in which pressure and density were assumed to be close to those corresponding to an adiabatically stratified atmosphere, and variations of potential temperature were neglected except when coupled with gravity. In this model we included a semi-grey treatment of radiation (constant absorption coefficients, but with different values for solar and thermal radiation). The thermal optical depth was taken as $\tau_T^* = 220$. When a large value of the solar optical depth was used, $\tau_S^* = 55$, so that solar radiation was absorbed near the top of the cloud layer (about 60 km), the circulation *did not* penetrate the atmosphere, but remained confined to the upper layers. In the lower atmosphere horizontal velocities were of the order of a few centimeters per second, and the advective terms were negligible in the thermal equation. When we allowed some penetration of solar radiation, $\tau_S^* = 2.3$, then "grid-size Bénard cells" appeared, making the results unreliable. This happened because the model lacked a mechanism to simulate the small-scale turbu-

[1] Presented at the Conference on the Atmosphere of Venus, Goddard Institute for Space Studies, 15–17 October 1974.

lent upward transport of heat that occurs when there is static instability.

These results seemed to imply that Goody and Robinson's dynamical model is not able to explain the high surface temperature. In the presence of a realistic density stratification and parameterization of radiation, the large-scale circulation driven by the heating contrast at the top of the cloud layer did not penetrate the lower atmosphere, which was therefore cooled down by longwave radiation. Unfortunately, the results were not conclusive enough, because of the short integration time, 4×10^7 s. One could not rule out the possibility that on a much longer time scale, of the order of the thermal relaxation time (10^9 s), the horizontal temperature gradients might diffuse down and be able to drive a deep circulation.

We have recently completed some other numerical experiments with the two-dimensional quasi-Boussinesq model, and obtained results that are much more conclusive. These results are presented in Section 2. We also include in this section some analytical radiative equilibrium solutions for a semi-grey atmosphere both with and without internal heating.

The two-dimensional models with solar heating averaged over a Venus day show not only a meridional Hadley cell, but also an indirect cell close to the pole. This is because at the top the rings of air coming from the equator approach the pole, conserving approximately their angular momentum; therefore, their zonal momentum increases until the centrifugal force is too strong, and the air is forced down. From this effect alone we should expect two types of regimes, at least for a quasi-two-dimensional circulation: a Hadley cell at low and middle latitudes and an indirect cell at high latitudes. The stronger the zonal velocities are at low and middle latitudes, the larger the indirect cell will be. Mariner 10 pictures have indeed shown essentially two regimes: at low and middle latitudes clouds spiraling toward the pole as in a Hadley cell, with zonal velocities increasing away from the equator, and polar rings and a polar cap at high latitudes (Murray *et al.*, 1974; Suomi, 1975). Of course, the perturbations associated with the subsolar region cannot be represented by a two-dimensional model.

The strong retrograde motion observed at high altitudes, with velocities of the order of 100 m s^{-1} even at the equator requires a nonsymmetrical mechanism to provide the upward transport of angular momentum necessary to compensate turbulent and viscous effects. We have developed and are currently testing a three-dimensional numerical model for Venus with the purpose of testing some of the theories that provide such a mechanism, especially those by Thompson (1970) and by Shubert and Whitehead (see Young and Schubert, 1973). A brief description of the model, and some preliminary results of the three-dimensional model are presented in Section 3. A two-dimensional version of this model was used to test the model proposed by Gierasch (1975) to explain the 4-day circulation, and these results are also presented in Section 3.

2. High surface temperature: Dynamical model versus the greenhouse effect

In order to make a more complete test of the validity of the dynamical model proposed by Goody and Robinson to explain the high surface temperature, we made some computations with different values of the effective solar optical depth, varying in this way the greenhouse effect.

a. Description of the model

The model used for these experiments was essentially the same as that described in Section 5 of Kálnay de Rivas (1973). It is a deep anelastic model, where the reference state is adiabatically stratified. The heating by the sun is averaged over a Venus day, and therefore there is no dependence on longitude. Rotation is included. There is a semi-grey treatment of radiation, with constant volume absorption coefficients, proportional to the mean adiabatic density and with different coefficients for solar and thermal radiation. In the computation of radiation we linearize departures from the basic adiabatic state. We use a vorticity type method of integration, i.e., the meridional equation of motion is replaced by a vorticity equation, thus eliminating pressure as a variable.

The most important change is that we included a mechanism for dry adiabatic adjustment in the case of an unstable stratification, to simulate, in a fashion similar to the one described by Manabe *et al.* (1965), the effect of small-scale convection: whenever $\partial\theta/\partial z < -\epsilon$ occurs, the temperature of the two layers where this happens is readjusted so as to keep the mean temperature of the two layers taken together constant (conserving the total potential energy) and to return to neutral stability. For this purpose, in the equation $T=T_{\rm ad}(z)+T'$ we assume $T'\approx\pi_{\rm ad}\theta'$, where T is the temperature, θ the potential temperature, $\pi=(p/p_0)^{R/c_p}$, the subscript ad refers to the mean adiabatic state, and the primes to the small departures from it. We take $\epsilon\approx10^{-4}$K km^{-1}, different from zero, to avoid redundant computations of the adiabatic adjustment processes. We also corrected the vertical diffusion and viscosity terms as indicated in Footnote 2 of Kálnay de Rivas (1973), but this change did not alter the results in any noticeable way.

b. Radiative equilibrium temperature and the greenhouse effect

In the semi-grey parameterization of radiation we assumed that the solar and thermal optical depths were proportional, i.e., $\tau_S=S\tau_T$ ($S=0$ corresponds to an atmosphere transparent to solar radiation). With this approximation, the radiative transfer equations

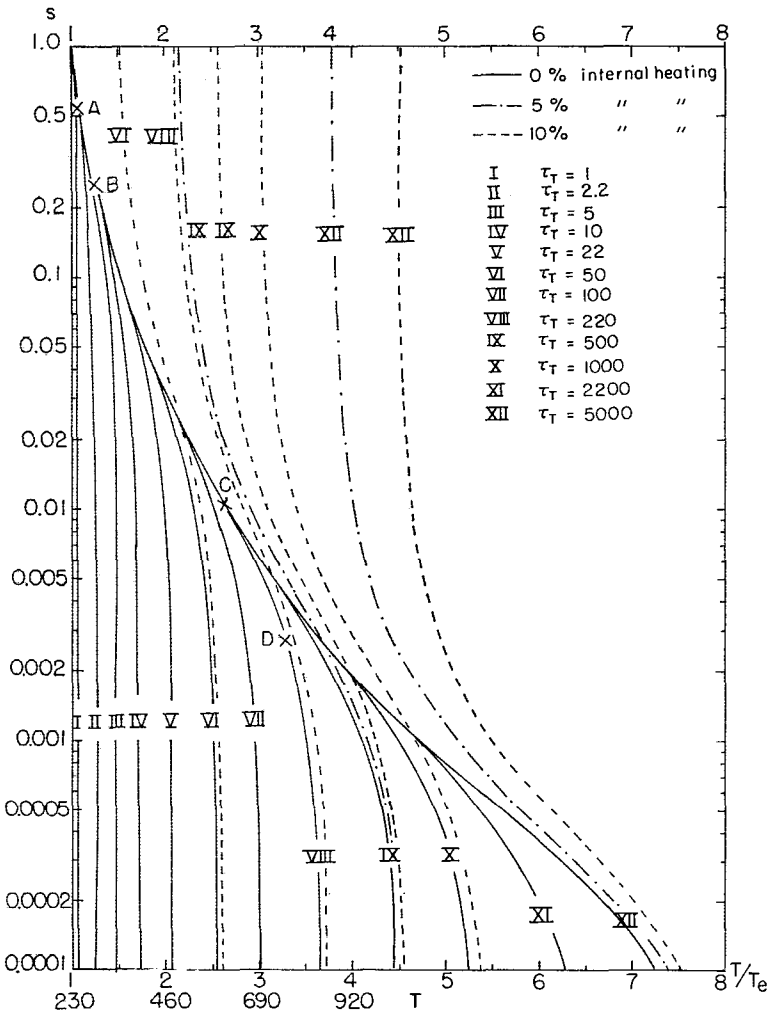

FIG. 1. Radiative equilibrium temperature as a function of the thermal optical depth τ_T and the ratio of the solar and thermal optical depths $S=\tau_S/\tau_T$. See text for further explanation.

[Gierasch and Goody, 1970, Eqs. (7) and (8)] can be integrated analytically in the case of radiative equilibrium where the net thermal flux is equal to the solar flux. If we also take into account the possibility of an internal source of heat, then the radiative equilibrium temperature T of the air is

$$T^4(\tau_T)=\frac{T_e^4}{2}\left[\frac{1+S}{S}-\left(\frac{1-S^2}{S}\right)\exp(-S r\tau_T)+c(r\tau_T+1)\right], \tag{1}$$

and similarly the temperature of the ground is

$$(T^*)^4=\frac{T_e^4}{2}\left[\frac{1+S}{S}+\left(1-\frac{1}{S}\right)\exp(-S r\tau_T^*)+c(r\tau_T^*+2)\right]. \tag{2}$$

Here T_e is the effective emission temperature, $r=1.66$ is a diffusivity factor, and we have assumed a normal solar flux $F_S=\sigma T_e^4$ and an internal heat source of intensity $G=c\sigma T_e^4$.

In Fig. 1 we show the ratio between the radiative equilibrium temperature of the air and the effective temperature for a wide range of values both of the thermal optical depth and $S=\tau_S/\tau_T$, for the case of no internal heating. We also plotted this ratio for the case in which there is an internal heat source with an intensity equal to 5% and 10% of the net thermal radiation, for selected values of τ_T. The radiative equilibrium temperature values corresponding to an effective temperature $T_e=230$ K, relevant to Venus, are also indicated.

It is clear that the surface temperature corresponding to an adiabatic stratification, $T\approx 750$ K, can only be attained under radiative equilibrium conditions, if $\tau_T^*\gg 100$ and $S\lesssim 0.005$. For example, if the solar optical depth is $\tau_S\approx 2$, a value which is compatible with the

TABLE 1. Radiative equilibrium temperature as a function of the solar and thermal optical depths. The top number corresponds to the case with no internal heating. The bottom number (in italics) corresponds to the case with an internal heating source whose intensity is 10% of the net thermal emission.

τ_T	τ_S 0.6	1	2.3	55
50	524	485	418	231
	536	*512*	*450*	*350*
220	759	708	604	288
	783	*735*	*650*	*485*
500	927	865	738	345
	968	*910*	*807*	*600*
1000	1105	1025	880	400
	1140	*1080*	*957*	*715*

Venera 8 observations (Avduevsky *et al.*, 1973), the thermal optical depth necessary to produce a sufficiently strong greenhouse effect is $\tau_T \gtrsim 500$. This conclusion is still valid if there is an internal heat source with an intensity compatible with the observations. Since the planetary albedo and the effective emission temperature are known with errors of the order of 5% (Hanel *et al.*, 1968; Gillett *et al.*, 1968; Irvine, 1968), then 10% is probably an upper limit to the intensity of any internal heat source. In Table 1 we show the radiative equilibrium temperature for some values of the thermal and solar optical depths, both for the case of no internal heating and 10% internal heating. We see that internal heating can be only of marginal importance, since the temperature increase that it produces is significant only for thermal optical depths so large that the greenhouse effect alone is enough to explain the high surface temperature.

The crosses on Fig. 1 (points A, B, C, D) correspond to combinations of τ_S^* and τ_T^* for which numerical experiments have been made.

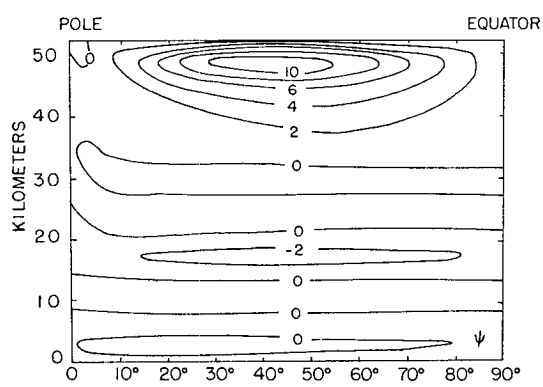

FIG. 2. Meridional mass streamfunction (10^4 g cm^{-1} s^{-1}) at the time $t=4\times10^7$ s (from Kálnay de Rivas, 1973). $\tau_S^*=55$. The vorticity-type model has been used.

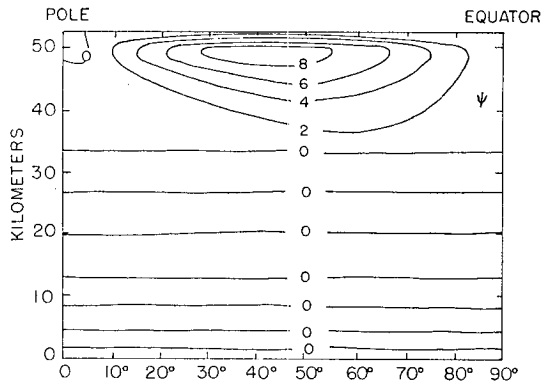

FIG. 3. As in Fig. 2 except at time $t=3\times10^8$ s.

c. Numerical experiments

We made different experiments keeping all physical parameters constant with the exception of the solar optical depth. The values of the physical parameters were as follows: horizontal and vertical coefficients of eddy viscosity and eddy diffusivity $\nu_H=K_H=10^{10}$ cm^2 s^{-1}, $\nu_V=K_V=10^4$ cm^2 s^{-1}; and total thermal optical depth $\tau_T^*=220$.

RUN I: Solar optical depth $\tau_S^*=55$ corresponding to point B in Fig. 1. This is the same as Run I in Kálnay de Rivas (1973), except that we integrated up to 3×10^8 s, a time comparable to the radiative time scale. Figs. 2 and 3 show the meridional mass streamfunction obtained after 4×10^7 s (from Kálnay de Rivas) and after 3×10^8 s. It is clear that the Hadley cell driven by the horizontal heating contrast at high levels *has not* penetrated further down. On the contrary, the main change is that the weak cells in the lower atmosphere induced by the initially discontinuous solar heating (the sun is "turned on" at time $t=0$) have disappeared almost completely. In the lower atmosphere horizontal velocities are ~1 cm s^{-1}. The lower atmosphere has been cooled down by radiation and has become more stable. The surface temperature has decreased by $\sim5\%$, or 37 K, which is close to the radiative-diffusive equilibrium temperature when radiation is parameterized as in the model, and the coefficient of vertical diffusivity is taken as $K_V=10^4$ cm^2 s^{-1} (see Kálnay de Rivas, 1971, p. 195).

RUN II: $\tau_S^*=2.3$ corresponding to point C in Fig. 1, or a radiative equilibrium temperature at the surface of 600 K. Fig. 4 shows the mass streamfunction after 3.2×10^7 s of integration. As could be expected, the Hadley cell is lower than in Run I, but *it still does not penetrate the lower atmosphere.* The base of the cell is located at about 20 km, and horizontal velocities are of the order of ~2 m s^{-1} above that level and ~2 cm s^{-1} below. The temperature at the surface is decreasing at almost the same rate as in Run I.

RUN III: $\tau_S^*=0.6$, with an attenuation coefficient $k=5$ above 36 km and $k=0.4$ below, simulating the

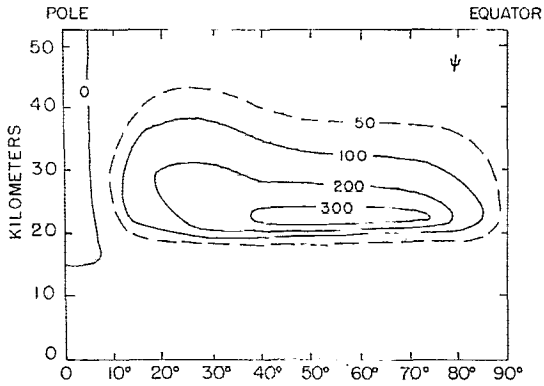

FIG. 4. As in Fig. 2 except for $\tau_S^*=2.3$. Time $=3.2\times10^7$ s.

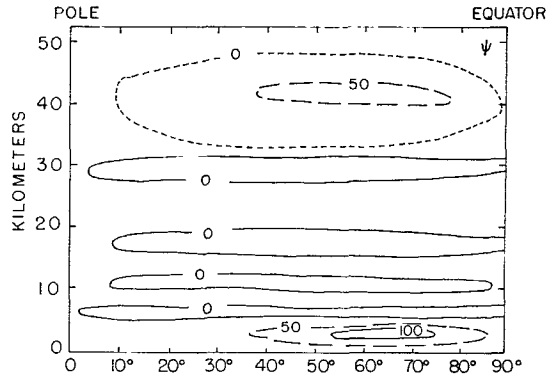

FIG. 6. As in Fig. 5 except $\partial\theta/\partial z=0.5$ K km^{-1} at time $t=0$.

stronger absorption due to clouds above 36 km (point D in Fig. 1). We ran two different cases with different initial conditions. In one case, neutral stability as in the previous runs, and in the other, positive static stability ($\partial\theta/\partial z=0.5$ K km^{-1}). Fig. 5 shows the mass streamfunction in the case of neutral initial stratification after 2.5×10^7 s, and Fig. 6 corresponds to the initially stable case after 2.2×10^7 s. The observed splitting of the Hadley cell is due to the discontinuity in the attenuation coefficient. In both cases there is a strong Hadley cell close to the surface, and horizontal velocities are about 2.5 m s^{-1}, except close to the surface where they become $\sim$50 cm s^{-1}. In the initially neutral case the surface temperature only decreased by 0.05% or 0.3 K, whereas in the initially stable case the surface temperature increased slowly so that the lapse rate became closer to the adiabatic lapse rate. The horizontal temperature contrast between equator and pole is about 2 K in the boundary layer next to the surface and $\sim$0.1 K in the interior.

3. The three-dimensional model for Venus

a. Description of the model

As indicated in the Introduction, a three-dimensional model has been developed and is currently being tested. Briefly, these are its characteristics: It is a quasi-Boussinesq "pressure type" model, i.e., we use the original momentum equations and determine the pressure through the solution of an elliptic equation. We use finite differences in the meridional plane (latitude and height) in order to be able to resolve boundary layers through the use of stretched coordinates. The longitudinal dependence is expanded in exponential Fourier components. Our goal is to resolve only the largest zonal scales, and when the number of modes is small (zonal wavenumber $\lesssim4$) the spectral method is as efficient as the finite-difference method, and much more accurate. The solar heating is also Fourier-analyzed, and the same number of zonal modes are retained as in the model. Adiabatic adjustment is realized by obtaining the potential temperature distribution at grid points regularly distributed in longitude, performing if necessary the temperature adjustment as described in Section 2, and transforming back to Fourier modes.

For the numerical integration we developed an energy conserving scheme, in order to avoid nonlinear instability. A staggered grid in the meridional plane was used, as shown in Fig. 7.

Other characteristics of the model and the parameterization of the physical processes are similar to those of the previously described two-dimensional "vorticity type" model.

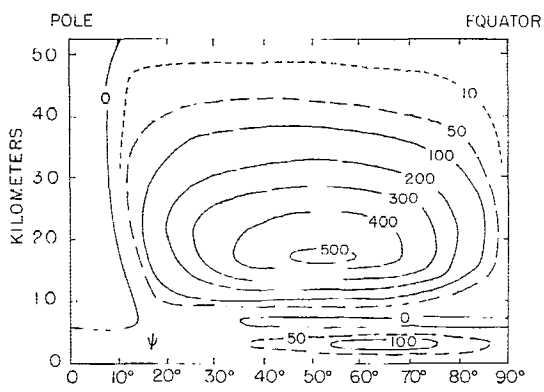

FIG. 5. As in Fig. 2 except for $\tau_S^*=0.61$. The attenuation coefficient is 11 times larger above 36 km than below. $\partial\theta/\partial z=0$ initially. Time $t=2.5\times10^7$ s.

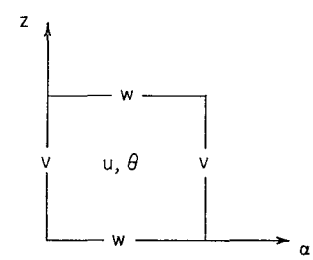

FIG. 7. Staggered grid in the meridional plane used in the three-dimensional model.

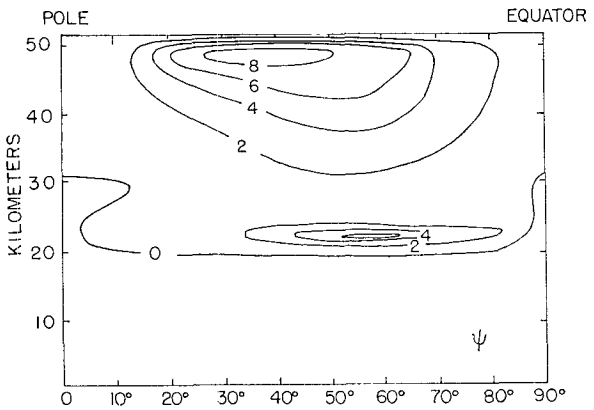

FIG. 8. Meridional mass streamfunction using a two-dimensional version of the three-dimensional model. $\tau_S^*=55$, $\tau_T^*=220$. The top is at $z=53$ km (300 mb).

b. Preliminary results: Two-dimensional runs

1) COMPARISON AND SENSITIVITY TEST RUNS

For the sake of comparison we tested the three-dimensional model with only zonal wavenumber 0 present. Even though the method of integration is quite different, the results were very similar to those obtained with the vorticity-type model. For example, Fig. 8 shows the meridional mass streamfunction obtained after 2.2×10^7 s for the same values of the physical parameters as in Run I of Section 2 (point B on Fig. 1). If we compare Fig. 2 with Fig. 8 we see that the only differences are that the transient weak cell in the interior is slightly stronger, and that the indirect polar cell is not present in Fig. 8. These differences are probably due to the lower resolution used in the pressure-type model (18 grid intervals between equator and pole versus 28 in the vorticity run). Even so, the maximum zonal velocity is the same as before (17 m s^{-1}) and also occurs at about 10° latitude away from the pole.

Other runs with different values of the solar optical depth gave results that were also very similar to the vorticity-type runs. When we used $\tau_S=0.6$ (point D in Fig. 1) with a constant attenuation coefficient, a single Hadley cell developed, but otherwise the results were similar to those described in Section 2.

In the previous runs the top of the model was taken at about 300 mb. To test the sensitivity of the results to the location of the upper boundary, we made another run with the top at 13 mb, and the solar and thermal optical depths $\tau_S^*=55$, $\tau_T^*=104$, respectively (point A in Fig. 1). As Fig. 9 shows, the Hadley cell center occurred at about the same height as in Run I (Fig. 8). The maximum velocities were similar to those in Run I (18 m s^{-1} and 12 m s^{-1} maximum zonal and meridional velocities), and also occurred at about 50 km, close to the center of the Hadley cell and not at the upper boundary. We conclude then that our numerical results are sensitive to the distribution of the heating but not to the location of the upper boundary.

We also tested the sensitivity of the results to the existence of a low-intensity internal heat source. We made a numerical experiment similar to Run I ($\tau_S^*=55$) and with the vertical coefficients of eddy viscosity and diffusivity equal to 10^3 cm^2 s^{-1}. Two separate runs were made, one with no internal heating and one with an internal heat source whose intensity was 5% of the net thermal radiation. In this case the radiative equilibrium temperature is 288 K without the source and 420 K with the source. The results of both runs were very similar. In both cases the circulation was like the one described as Run II (Fig. 7a in Kálnay de Rivas, 1973) i.e., the Hadley cell remained in the upper atmosphere. The only difference was that the decrease of the surface temperature from its initial value of 730 K was 20% faster in the case of no internal heating than in the case of a 5% intensity internal heating.

2) RUNS TESTING GIERASCH'S MECHANISM

Gierasch (1975) has proposed a new mechanism to explain the 4-day circulation. It is assumed that there is strong horizontal diffusion and weak vertical diffusion, faster and slower, respectively, than the meridional overturning. Therefore, the horizontal diffusion will produce a velocity distribution close to solid rotation at each level, and a meridional Hadley cell will transport angular momentum upward at a rate fast enough to compensate for vertical diffusion. The zonal winds generated at high levels can be in cyclostrophic balance against the meridional pressure gradient. Zonal velocities of $\sim$100 m s^{-1}, as observed at the equator, are compatible with cyclostrophic balance if the equator-to-pole temperature contrast is of the order of 3 K throughout the atmosphere (Leovy, 1973).

The time scale of the meridional overturning of the Hadley cell is $t\sim L/v=10^7$ s where $L=10{,}000$ km is the distance from equator to pole, and $v=1$ m s^{-1} the

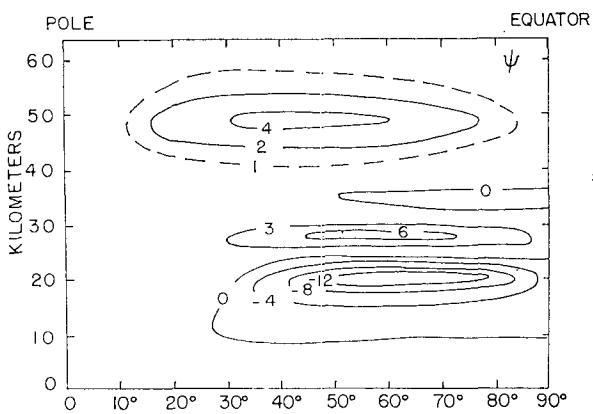

FIG. 9. As in Fig. 8 except that $\tau_T^*=104$, and the top is at 63 km (13 mb).

typical meridional velocity. Therefore the mechanism suggested by Gierasch requires horizontal eddy diffusion coefficients larger than 10^{11} cm^2 s^{-1}, and vertical coefficients smaller than 10^5 cm^2 s^{-1}. Gierasch suggests baroclinic instability associated with relative rotation as a phenomenon that might produce such strong horizontal mixing.

We have performed several two-dimensional numerical experiments to test the validity of this mechanism. We used in every case a value of 10^4 cm^2 s^{-1} for the vertical coefficients of eddy viscosity and diffusivity, and a solar optical depth $\tau_S^*=2.3$.

When we used horizontal coefficients of eddy viscosity and diffusivity $\nu_H=K_H=10^{12}$ cm^2 s^{-1}, the main effect of the strong horizontal diffusion was to reduce the horizontal temperature contrast to 0.01 K (compared to 0.2 K for the case in which $\nu_H=K_H=10^{10}$ cm^2 s^{-1}). Consequently, the meridional cell slowed down, so that after 1.5×10^7 s the maximum zonal and meridional velocities were 0.4 and 8 cm s^{-1} respectively (compared to maximum velocities of 10 m s^{-1} in both directions for the case in which $\nu_H=K_H=10^{10}$ cm s^{-1}). When we assumed $\nu_H=K_H=10^{11}$ cm^2 s^{-1}, the maximum zonal and meridional velocities were 1.5 and 2.6 m s^{-1} respectively, after 1.8×10^7 s of integration. Similar velocities were observed after the first 10^7 s of integration when we started from a state of solid rotation, with $u=20$ m s^{-1} at the equator. In all these cases, at the end of the period of integration the intensity of the circulation was slowly *decreasing* with time.

When we used a Prandtl number larger than 1, $\nu_H=10^{11}$ cm^2 s^{-1} and $K_H=10^9$ cm^2 s^{-1}, the maximum zonal and meridional velocities were 4 and 6 m s^{-1} respectively after 3×10^7 s of integration. The same results were obtained both when we started from a state of solid rotation with $u=20$ m s^{-1} at the equator and when we used $\nu_H=10^{11}$ cm^2 s^{-1} and $K_H=10^{10}$ cm^2 s^{-1}. When we used $\nu_H=10^{12}$ cm^2 s^{-1} and $K_H=10^{10}$ cm^2 s^{-1} then the maximum zonal and meridional velocities were 30 cm s^{-1} and 4 m s^{-1} respectively. In all these cases the zonal velocity at the equator was of the same order as the maximum zonal velocity, whereas in the case in which $K_H=\nu_H=10^{10}$ cm^2 s^{-1}, it was only $\sim$40 cm s^{-1} at the equator and $\sim$10 m s^{-1} in middle latitudes.

c. Preliminary results: Three-dimensional runs

We are starting to test the three-dimensional version of the model. We ran cases in which only zonal wavenumbers 0 and 1 were present. We found that a rather unsmooth circulation, with small-scale structure in the meridional plane and winds of the order of 20 m s^{-1} developed. At present we are studying whether these results are due to a physical instability or to some fault of the model.[2]

[2] R. Young (personal communication) has observed similar results. In his three-dimensional spectral model for Venus the highest wavenumber present contained the maximum energy.

4. Summary and conclusions

We have presented results proving that only the greenhouse effect can explain the high surface temperature observed on Venus. When the thermal and solar optical depths are such that the radiative equilibrium temperature is smaller than the observed surface temperature, the meridional Hadley cell does not penetrate the lower atmosphere which is then cooled down by radiation. Very long integrations, up to a time comparable with the radiative relaxation time, have confirmed this result. When the greenhouse effect is large enough to produce radiative equilibrium surface temperatures at least as large as the observed values, then the large-scale circulation penetrates the whole atmosphere. In this case the lapse rate is maintained close to the adiabatic value, in agreement with the Mariner 5 and Venera observations (Marov *et al.*, 1973). Goody and Robinson's hypothesis that a Hadley cell driven by the solar heating contrast at the top of the atmosphere would convect heat downward and maintain an adiabatic lapse rate is therefore not valid. This result agrees with the argument presented by Stone (1974, 1975) that a Hadley cell, being a direct circulation, can only transport heat upward. The order of magnitude of the horizontal and vertical velocities and horizontal temperature gradient in the deep atmosphere, in the case of sufficient greenhouse effect, agree extremely well with those estimated through scale analysis by Stone (1974, 1975). In the upper atmosphere the maximum zonal velocities induced by a two-dimensional circulation are 10–20 m s^{-1}.

We presented semi-grey radiative equilibrium calculations for a wide range of solar and thermal optical depths. Similar calculations were made including an internal heat source with intensity compatible with observations (10% of the net thermal flux). These calculations show that an internal heat source cannot account by itself for the high surface temperature. A numerical experiment in which a 5% internal heat source was included confirmed this result. The radiative equilibrium calculations show that if the solar optical depth is about 2, a result compatible with the Venera 8 observations, then a thermal optical depth of at least 500 is required to provide enough greenhouse effect.

Numerical experiments show that the mechanism proposed by Gierasch (1975) to explain the 4-day circulation does not work if the horizontal Prandtl number ν_H/K_H is O(1). This happens because the strong horizontal diffusion will eliminate most of the horizontal temperature gradient. Horizontal eddy diffusion coefficients larger than $K_H=10^{10}$ cm^2 s^{-1} will considerably reduce the horizontal temperature gradient required to drive the meridional Hadley cell. Gierasch's mechanism, on the other hand, requires a horizontal eddy viscosity coefficient $\nu_H\gtrsim10^{12}$ cm^2 s^{-1}, so that it may work only if the Prandtl number is O(100) or

larger. However, numerical experiments using a large Prandtl number failed to show increased zonal velocities. The reason for this failure is the following: the effect of horizontal diffusion coefficients is not only to make approximately uniform the distribution of angular velocity with altitude, as stated by Gierasch, but also to *dissipate* angular momentum. In our numerical results this dissipation was the dominant effect, and it more than compensated for the upward transport of angular momentum due to the meridional Hadley cell.

Preliminary three-dimensional calculations show a tendency to develop strong small-scale circulations.

Acknowledgments. I wish to thank Profs. P. Stone and R. Prinn and Mr. J. Roads for some useful discussions. The computations were performed at the National Aeronautics and Space Administration (NASA) Goddard Institute for Space Studies under NASA Grant NGR 22-009-727. This work was supported by NASA under Contract NAS2-7994 and by the National Science Foundation under Grant A 28724X.

REFERENCES

Avduevsky, V., M. Marov, B. Moshkin and A. E. Ronomov, 1973: Venera 8: Measurements of solar illumination through the atmosphere of Venus. *J. Atmos. Sci.*, **30**, 1215–1218.

Gierasch, P., 1975: Meridional circulation and the maintenance of the Venus atmospheric rotation. *J. Atmos. Sci.*, **32**, 1038–1044.

——, and R. M. Goody, 1970: Models of the Venus clouds. *J. Atmos. Sci.*, **27**, 224–245.

Gillett, F. C., F. J. Low and W. A. Stein, 1968: Absolute spectrum of Venus from 2.8 to 14 microns. *J. Atmos. Sci.*, **25**, 594–595.

Goody, R., and A. Robinson, 1966: A discussion of the deep circulation of the atmosphere of Venus. *Astrophys. J.*, **146**, 339–353.

Hanel, R., M. Forman, G. Stambach and T. Meilleur, 1968: Preliminary results of Venus observations between 8 and 13 microns. *J. Atmos. Sci.*, **25**, 586–593.

Irvine, W. M., 1968: Monochromatic phase curves and albedos for Venus. *J. Atmos. Sci.*, **25**, 610–616.

Kálnay de Rivas, E., 1971: The circulation of the atmosphere of Venus. Ph. D. thesis, Dept. of Meteorology, MIT.

——, 1973: Numerical models of the circulation of the atmosphere of Venus. *J. Atmos. Sci.*, **31**, 763–779.

Leovy, C., 1973: Rotation of the upper atmosphere of Venus. *J. Atmos. Sci.*, **30**, 1218–1220.

Manabe, S., J. Smagorinsky and R. F. Strickler, 1965: Simulated climatology of a general circulation model with a hydrologic cycle. *Mon. Wea. Rev.*, **93**, 769–798.

Marov, M., V. Avduevsky, V. Kerzhanovich, M. Rozhdestvensky, N. Borodin and O. Ryabov, 1973: Venera 8: Measurements of temperature, pressure, and wind velocity on the illuminated side of Venus. *J. Atmos. Sci.*, **30**, 1210–1214.

Murray, G., M. Belton, G. Danielson, M. Davies, D. Gault, B. Hapke, B. O'Leary, R. Strom, V. Suomi and N. Trask, 1974: Venus: Atmospheric motion and structure from Mariner 10 pictures. *Science*, **183**, 1307–1315.

Pollack, J., 1969: A nongrey CO_2-H_2O greenhouse model for Venus. *Icarus*, **10**, 314–341.

Sagan, C., 1962: Structure of the lower atmosphere of Venus. *Icarus*, **1**, 151–169.

Stone, P., 1974: The structure and circulation of the deep Venus atmosphere. *J. Atmos. Sci.*, **31**, 1681–1690.

——, 1975: The dynamics of the atmosphere of Venus. *J. Atmos. Sci.*, **32**, 1005–1016.

Suomi, V., 1975: Mariner 10 observations of cloud motions. Presented at the Conference on the Atmosphere of Venus.

Thompson, R., 1970: Venus' general circulation is a merry-go-round. *J. Atmos. Sci.*, **27**, 1107–1116.

Young, R., and G. Schubert, 1973: Dynamical aspects of the Venus 4-day circulation. *Planet. Space Sci.*, **21**, 1563–1580.